Diffusion in binary gas mixtures studied by NMR of hyperpolarized gases and molecular dynamics simulations

R. H. Acosta,† L. Agulles-Pedrós, S. Komin, D. Sebastiani, H. W. Spiess and P. Blümler‡

Received 30th June 2006, Accepted 31st July 2006
First published as an Advance Article on the web 14th August 2006
DOI: 10.1039/b609316g

The dependence of the individual mean square displacement of rare gases in binary mixtures is studied by a combined experimental and theoretical approach. We show that the diffusion constant can be varied in a considerable range by changing the molar fractions of the mixtures. On the experimental side, NMR diffusion measurements are done on hyperpolarized ^{3}He and ^{129}Xe, mixed with several inert buffer gases, in the presence of a magnetic field gradient. The results are compared to diffusion coefficients obtained from atomistic molecular dynamics simulations based on Lennard-Jones type potentials of the corresponding gas mixtures, and to appropriate analytical expressions, yielding very good mutual agreement. This study is the first quantitative validation of the effects of the mutual interactions between gas particles on the individual diffusion properties. It is shown that the dependency of gas phase diffusion properties on the local chemical environment may not be neglected, *e.g.* in diffusion-controlled chemical reactions.

Introduction

From the very beginning of the application of laser-polarized (LP) noble gases (^{3}He and ^{129}Xe) to magnetic resonance imaging (MRI), diffusion measurements were envisioned as a tool for studying the microscopic structure of respiratory organs.[1,2] This is possible because the NMR signal acquired in the presence of a magnetic field gradient is attenuated exponentially with the diffusion coefficient. However, in the case of liquids, the diffusion coefficient is on the order of 10^{-8}–10^{-9} m^2 s^{-1}, which limits the spatial resolution to about 10 μm.[3] Diffusion coefficients of gases at standard temperature and pressures are of the order of 10^{-4}–10^{-5} m^2 s^{-1}, which are 4–5 orders of magnitude greater than in liquids. At first glance, these fast rates should significantly reduce the spatial resolution; however, there are two effects in lung imaging which reduce the influence of diffusion. Although the distance diffused during a typical time interval of 1 ms for the application of a gradient pulse is approximately 600 μm for ^{3}He gas, the diffused distance will be reduced by the restrictions imposed by the dimension of the volume, giving rise to an apparent diffusion coefficient (ADC).[4–6] The second condition that influences the diffusion coefficient of the noble gas is its interaction with other gases present in the imaged volume, typically N_2 and O_2 in biomedical applications. The diffusion coefficient in a mixture has in general been calculated based on the Chapman–Enskog theory as a function of partial pressures[7–9] or measured for samples with an increasing overall pressure.[8,10–12]

In order to improve the quality of gas MRI most attempts have lead to optimizations of pulse sequences, with the fundamental aim to shorten and weaken the gradient pulses, thus reducing the attenuation of the NMR signals due to diffusion as much as possible. This approximation is limited due to the required spatial resolution and technical limits for the switching time of gradients. Another approach is to influence the diffusion coefficient by admixing with an inert buffer gas, hence reducing the LP gas diffusion coefficient, which results in an increase in sensitivity and therefore resolution. This approach was first explored with admixtures of LP-^{129}Xe and sulfur hexafluoride (SF_6), although no noticeable effect was obtained due to the comparable diffusion coefficients.[10] Experimental evidence of sensitivity enhancement in the trachea of dissected mice lungs was shown recently for a mixture of LP-^{3}He with LP-^{129}Xe at varying pressures.[13]

In this work we explore the possibility of generating a highly controlled binary gas mixture with 1 bar overall pressure, which is a necessary condition for clinical imaging. The diffusion coefficient of the mixture as a function of the relative gas concentration is used to show the accuracy in the gas mixing. The purpose of this paper is the detailed description of our solution to the problems arising when mixing small amounts of gases of different molecular mass and determining the diffusion coefficient of one (the NMR-sensitive) isotope. In the course of the experiments it turned out that NMR was the most precise way to determine the gas concentrations. Originally it was intended to use independent analytical techniques (*e.g.* mass spectroscopy, gravimetry or partial pressures) to determine the concentrations, but since different helium isotopes were used, quantification even within a few percent was

Max-Planck Institute for Polymer Research, Mainz, Germany
† Present address: Facultad de Matemática, Astronomía y Física, Universidad Nacional de Córdoba, X5016LAE, Córdoba, Argentina.
‡ Present address: Institute of the Chemistry and Dynamics of the Geosphere, ICG-III: Phytosphere, Research Center Jülich, 52425 Jülich, Germany. E-mail: p.bluemler@fz-juelich.de.

 This journal is © the Owner Societies 2006

not possible with the available equipment. Hence, a method for mixing gases and determining the molar fractions and diffusion coefficients had to be devised and is presented in the following.

A detailed description of the gas handling setup as well as the theory for the precise determination of the molar fraction of ^{3}He and ^{129}Xe in admixture with different buffer gases is presented in the first section. The resulting protocol is applied for the measurement of the diffusion coefficient as a function of the molar fraction for three very different buffer gases, namely ^{4}He, N_2 and SF_6. The admixture of LP-^{3}He with these gases is very relevant; ^{4}He and SF_6 are very light and very dense gases, respectively. It has been shown that they can be used to provide opposite contrasts,[14] while N_2 is present in most biological studies. The inverse situation of a dense LP gas such as ^{129}Xe upon a mixture with ^{3}He was also studied.

We have also performed direct atomistic molecular dynamics simulations on the binary gas mixtures in order to obtain a realistic theoretical description of the diffusion properties of our systems at the actual temperature and pressure of the corresponding experiments. Using interaction potentials of Lennard-Jones type, our molecular dynamics simulations incorporate the mass and size of the individual particles as well as their mutual attraction and repulsion due to the interactions of the electronic clouds of the atoms.

Experimental

NMR setup and LP-gas delivery

All data were acquired in a 4.7 T horizontal, 20 cm bore magnet (Magnex Scientific Ltd, UK) equipped with actively shielded gradients (capable to produce gradients up to 0.3 T m^{-1}) from Bruker (Bruker Biospin GmbH, Germany). The gradients were driven by amplifiers from Copley (Copley Controls Corp., USA). A birdcage-coil of 21 mm inner diameter and 37 mm length from Bruker was used for RF excitation and detection at a frequency of 153.096 MHz for ^{3}He. The gradients and the RF were controlled from a Maran DRX console (Resonance Instruments Ltd, Witney, UK) controlled from within a Matlab (MathWorks Inc., USA) environment by self developed software.

The ^{3}He polarization was carried out using a home built large scale polarizer located at the department of Physics in the University of Mainz, which can produce up to 70% of polarization at 3.3 bar l h^{-1} and 80% at 1.2 bar l h^{-1}.[15] The polarization process is based on the metastable spin exchange method.[1,16] Typically transport cells of iron-free glass (Supremax glass, Schott, Mainz, Germany) with a volume of 1.2 L, were filled with 2.1–2.7 bars of 60–70% LP-^{3}He. Subsequently, the cells were placed in a shielded container with a low magnetic field (0.8 mT) produced by permanent magnets[15] and transported to the MRI Laboratory in the Max Planck-Institute. The helium was then stored in a very homogeneous magnetic field of 2.5 mT, generated by five coaxial coils of 45 cm diameter and 70 cm total length.

Optical polarization of xenon was achieved using an apparatus designed and constructed by S. Appelt and coworkers at the Research Center Jülich, Germany,[17] located in the Max Planck-Institute for Polymer Research, Mainz. A gas mixture consisting of 1% of Xe (natural isotope distribution), 5% N_2 and 94% ^{4}He was used for LP of ^{129}Xe. LP-xenon was frozen and collected by immersion in a liquid nitrogen bath in the bore of a magnet consisting of an arrangement of 16 permanent bar-magnets in a Halbach configuration producing a magnetic field of 0.3 T.[18] The polarization was measured to be higher than 30%.

Gas handling and mixing

In order to prepare gas mixtures in a controlled way a dedicated setup for the gas handling had to be designed which is schematically presented in Fig. 1. A sample tube of volume V filled with LP-gas was connected to port D of the gas handling system, which is already positioned inside the NMR magnet. For ^{3}He measurements the sample tube was pre-evacuated and filled directly from the transport cell. Xenon filled bottles were pre-evacuated after a 10 min accumulation of solid hyperpolarized xenon and then connected to port D of the gas handling system; the bottle was left to reach ambient temperature for a period of approximately 10 min under the presence of air flow.

Valves A, B and C are pneumatic piston-valves (Festo AG and Co. KG, Esslingen Germany) which were modified to replace all magnetic components. In turn these are controlled by Festo magnetic air valves driven by the spectrometer console. In this way the mixing procedure could be completely automated and synchronized to the pulse sequences.

In order to minimize the length of the connection lines the pneumatic valves are located in the bore of the magnet in direct vicinity to the sample tube inside the RF coil. To complete the setup a non magnetic pressure sensor (Sensortechnics GmbH, Puchheim Germany, PCB Series) was used to monitor the whole procedure. This sensor was also placed in the bore of the magnet and has an accuracy of 1 mbar. Ambient pressure was measured to be P_A = 975 mbar in all the experiments.

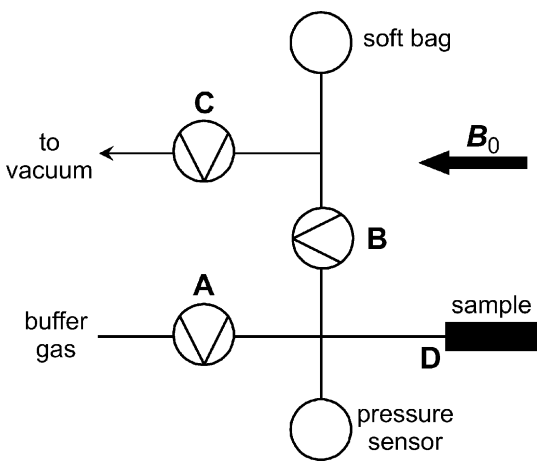

Fig. 1 Sketch representing the pneumatic valve configuration used for preparing the different gas mixtures. A, B and C are pneumatic valves that are controlled from the spectrometer console. See text for details of their operation.

Valves B and C are opened in order to evacuate the transmission line to values in the order of 10^{-6} bar. Once B and C are closed, the sample tube is opened to let the LP-gas expand into the transmission line. Valve B is then opened during a time t_B to release the exceeding pressure to a large soft bag, thus establishing ambient pressure, P_A, of LP-gas in the sample tube. The ambient pressure is used as a reference pressure for all experiments. Closing B and opening C for a period of t_C permits the evacuation of the soft bag. The buffer gas is then pressed into V by opening valve A for a short period of time, t_A. Prior to the equilibration with P_A an experimentally determined waiting time of 6 s is introduced to assure equilibrium in the gas mixture. At this point it is worth to note that mixing of gases is not due to diffusion processes as this would involve very long waiting times. The pressure of the buffer gas reservoir was typically set to 3 times P_A, in this way a turbulent inflow is generated which produces a complete mixture of both gases. The stabilization of the pressure sensor oscillated in 3–4 s, and the diffusion coefficient was measured repeatedly for a single inflow with a waiting time up to 10 min with no apparent change within the experimental error.

A reservoir with pressures of about 2.5 bar was used for the different buffer gases mixed. t_A was set to 900 ms for SF_6 and xenon and to 400 ms for N_2, ^{4}He and ^{3}He. t_B and t_C were fixed to values of 2 s and 500 ms, respectively for all experiments.

Diffusion measurement

Diffusion measurements were carried out using a pulsed gradient echo sequence (PGE)[19] with trapezoidal bipolar gradients; the used timings and nomenclature are shown in Fig. 2. Two acquisitions for ten b-values were accumulated by stepping the diffusion gradient intensity, where b is obtained from the Stejskal–Tanner equation[20] modified to take the shape of the gradients[6] into account

$$\ln\frac{S(b)}{S(0)} = -bD \text{ with } b = \gamma^2 G^2\left(\frac{2}{3}\delta^3 + \frac{\varepsilon^3}{30} - \frac{\delta\varepsilon^2}{6}\right). \qquad (1)$$

S is the NMR signal intensity, γ is the gyromagnetic ratio, δ = 500 μs and ε = 50 μs and D is the diffusion coefficient. The maximum diffusion gradient strength, G_{max}, was 0.06 T m^{-1}. A hard RF pulse with duration of 5 μs was used, which corresponds to a tip angle of $\alpha \approx 3°$. The sequence was repeated as fast as possible due to the non-equilibrium nature

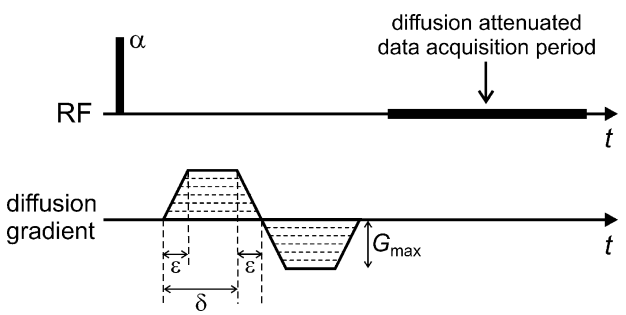

Fig. 2 Schematic representation of the pulse sequence introducing the used nomenclature. Top row: timing of RF excitation and acquisition; bottom row: diffusion gradient.

of the spin polarization (no repetition delay). With these experimental conditions the deviation was less than 5% for each diffusion measurement obtained from the linear fits following eqn (1).

Determination of the molar fractions

Initially a pressure P_A of LP-^{3}He is contained in the sample tube, having a total number of k moles in a volume V. When m_1 moles of a buffer gas (BG) are pressed into the same volume V, the helium is diluted by a factor f_1, which in this case is the same as the ^{3}He molar fraction,

$$x_1 = f_1 = \frac{k}{k + m_1}. \qquad (2)$$

As described above, the pressure is then released to P_A. However, this leaves the molar fraction unchanged, so that the remaining number of LP-^{3}He moles in volume V follows the relation $x_1 = k_1/k$, which can be rewritten as

$$k_1 = kx_1 = \frac{k^2}{k + m_1}. \qquad (3)$$

With the same reasoning the molar fraction of BG does not change when valve B is opened, so that the number of moles, m_1', of BG remaining in V are given by

$$x_{BG} = \frac{m_1'}{k} = \frac{m_1}{k + m_1} \qquad (4)$$

or

$$m_1' = \frac{km_1}{k + m_1}. \qquad (5)$$

When the procedure is repeated, that is, when m_2 moles of BG are pressed in V, the new ^{3}He molar fraction will be

$$x_2 = \frac{k_1}{k_1 + m_1' + m_2}. \qquad (6)$$

By substituting eqn (3) and (5) into the last equation the following expression is obtained,

$$x_2 = x_1 f_2 \qquad (7)$$

where $f_2 = k/(k + m_2)$ can be thought of as the dilution of the gas mixture corresponding to x_1 by the addition of m_2 moles of BG. For the nth experiment this can be generalized as

$$x_n = \prod_{i=1}^{n} f_i = \prod_{i=1}^{n} \frac{k}{k + m_i} \qquad (8)$$

where f_i is the dilution of the gas mixture corresponding to the ith step.

As the determination of the molar fractions will be carried out by inspection of the NMR signal it is necessary to combine the equations above with the evolution of the magnetization during the measurement of each mixing step. Initially, for pure LP-^{3}He at P_A, the magnetization is M_0. However, N excitations of the non-equilibrium magnetization will be carried out in each experiment (in this example 10 gradient amplitudes with two scans in which the phase was cycled to correct for possible base line artifacts; resulting in a total number, N = 20, of RF pulses). This will reduce the magnetization

 This journal is © the Owner Societies 2006

additionally to

$$\tilde{M}_1 = aM_0 \tag{9}$$

where $a = \cos^{N-1}(\alpha)$.[21–23] Relaxation due to the walls of the sample will be ignored as the total duration of the experiment is less than 10 min, while the typical relaxation times of the used samples were measured to be longer than 10 h. After BG is pressed into the sample and the exceeding pressure is released to P_A, the magnetization will become

$$M_1 = aM_0 f_1 = aM_0 x_1. \tag{10}$$

If this is repeated for a second time as described above, the magnetization will become

$$M_2 = aM_1 f_2 = a^2 M_0 x_2, \tag{11}$$

this expression can be generalized for the nth experiment as

$$M_n = a^n M_0 x_n. \tag{12}$$

The signal acquired will be $S_n = M_n \sin(\alpha)$, hence the following expression is used to obtain the helium molar fractions from the measurement of the actual magnetization (*e.g.* a reference signal)

$$x_n = \frac{S_n}{a^n S_0}, \tag{13}$$

where S_0 is the initial NMR signal acquired.

From eqn (13) it is clear that an imperfection in the pulse angle determination will scale as a power of the number of experiment, therefore its determination must be done very accurately. Another aspect of the setup that can have influence on the molar fraction determination is a small residual volume that lies between the volume of the sample contained inside the RF coil and valves A and B. The polarization of the gas present in this volume will not be affected by the RF pulse, hence leading to a systematic error in the molar fraction determination. This volume was minimized as far as possible and determined to be 5% of the volume contained inside the RF coil. The pulse tip angle was determined by running the whole sequence for measuring $D(x)$ with pure LP-gas and setting the factor a so that the molar fraction calculated was equal to unity. The error in the tip angle was determined to be lower than $\Delta\alpha = 5\%$. However, this error propagates during the course of the experiments (n mixtures excited by N RF pulses each). Error propagation of eqn (13) results in an error Δx_n of the determined molar fraction x_n of the LP-^{3}He as

$$\frac{\Delta x_n}{x_n} = n(N-1)\tan\alpha\,\Delta\alpha \tag{14}$$

assuming that the error on the measured NMR-signals is much smaller. The biggest error in the presented data is therefore about 8% for the last molar fraction in the ^{3}He/SF_6 mixture (*cf.* horizontal error bars in Fig. 4.)

Molecular dynamics simulations

Classical molecular dynamics simulations under periodic boundary conditions have been carried out using the Gromacs simulation package.[24] We have simulated ^{3}He upon a mixture with ^{4}He, N_2 and ^{129}Xe as buffer gases at molar fractions from 0 to 1 in steps of 0.1.

Atoms were modeled using pairwise 6–12 Lennard-Jones potentials:

$$V = 4\varepsilon((\sigma/r)^{12} - (\sigma/r)^6) \tag{15}$$

with $r = |R_1 - R_2|$. N_2 was represented as a united atom. The Lennard-Jones parameters ε and σ were taken from ref. 25. Their values are ε(Xe) = 231 K, σ(Xe) = 4.047 Å, ε(He) = 10.22 K, σ(He) = 2.551 Å, $\varepsilon(N_2)$ = 71.4 K, $\sigma(N_2)$ = 3.798 Å. For interactions between particles of different species, the combination formulae

$$\sigma_{ij} = (\sigma_i + \sigma_j)/2; \quad \varepsilon_{ij} = \sqrt{\varepsilon_i \varepsilon_j} \tag{16}$$

were used.

For the thermodynamic parameters of the binary gas mixtures, the equation of state of an ideal gas was assumed. In order to match the experimental pressure and temperature, simulation boxes of 205 379 nm^3 = (59 nm)^3 containing 5000 particles were used for the ^{3}He–^{4}He and ^{3}He–^{129}Xe mixtures. A check on the equivalent systems with only 500 particles yielded only insignificant deviations from the corresponding 5000 particle runs. Hence, we used only 500 particles for the ^{3}He–N_2 system. For the equilibration of our systems, the particles were placed at random positions in the box and brought to the desired temperature (T = 294 K) by a canonical (NVT) molecular dynamics run for 20 ps. Subsequently, production runs of 10 ns length were performed in the NVE ensemble, with a time step of 2 fs.

Diffusion coefficients were computed from the production runs by fitting the root mean square displacement, averaged over all atoms of a given species i, to the elapsed time, assuming the Einstein–Smolochowski relation

$$\langle R_i(T) - R_i(0)\rangle^2 = 6D_i T. \tag{17}$$

Error bars were estimated by comparing the diffusion coefficients obtained from the first and second half of the simulation. The simulations were performed on a parallel 16-processor Beowulf cluster with 2.6 GHz Xeon processors and required about 2000 CPU hours in total.

Results and discussion

Since the method of mixing and expanding gas mixtures while measuring diffusion coefficients could have inherent faults (*e.g.* leakage, depolarization *etc.*) the robustness and reliability of the method is demonstrated in Fig. 3. The normalized diffusion attenuated signal is plotted *versus* the b-value for a high concentration, x = 1 (pure helium) and a relatively low concentration, x = 0.13 of ^{3}He in a binary mixture with SF_6. The straight lines correspond to a linear regression of eqn (1), which yield diffusion coefficient values of $D_{He} = 1.85 \times 10^{-4}$ m^2 s^{-1} for pure ^{3}He (x = 1) and $D_{He/SF_6}(0.13) = 5.3 \times 10^{-5}$ m^2 s^{-1} for the binary mixture. The standard deviation uncertainties resulting from the statistical error in the regression analysis are less than 5% for all the measurements shown in this work.

Fig. 4 shows the inverse of the diffusion coefficient of ^{3}He as a function of its molar fraction for four different BG ($D_{He/BG}(x)$). The free diffusion coefficient of a gas in a mixture is usually written as a function of reduced diffusion coefficients

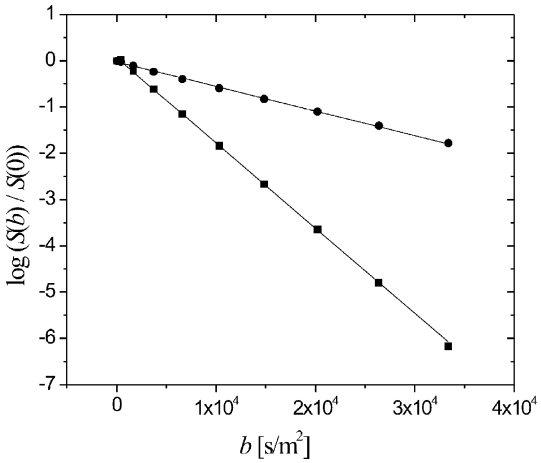

Fig. 3 Demonstration of the pulsed gradient technique used for the diffusion measurements. The Stejskal–Tanner echo attenuation semi-log plot described in eqn (1) is shown for two ^{3}He molar fractions upon an admixture with SF_6 (■ for $x = 1$ and ● for $x = 0.13$), yielding diffusion coefficients of 1.85×10^{-4} m^2 s^{-1} and 5.3×10^{-5} m^2 s^{-1}. The maximum b-value corresponds to a diffusion gradient strength of 0.06 T m^{-1}. The gradient timings were $\delta = 500$ μs and $\varepsilon = 50$ μs.

that take into account the partial pressures in the mixture.[7–10] As all the experiments presented in this work are performed at an overall pressure of ~1 bar, an analogous description that takes into account the ^{3}He molar fraction is used

$$\frac{1}{D_{\mathrm{He/BG}}(x_{\mathrm{He}})} = \frac{x_{\mathrm{He}}}{D_{\mathrm{He}}} + \frac{1 - x_{\mathrm{He}}}{D^0_{\mathrm{He/BG}}}, \qquad (18)$$

where D_{He} is the self diffusion coefficient of ^{3}He and $D^0_{\mathrm{He/BG}}$ is the binary diffusion coefficient of the ^{3}He/BG system and can be found by extrapolating to $x_{\mathrm{He}} = 0$. The solid lines in Fig. 4 correspond to a fit of eqn (18) to the individual data sets.

The simulated dependence of the binary diffusion coefficients in the ^{3}He–^{4}He, ^{3}He–N_2 and ^{3}He–^{129}Xe mixtures on x_{He} is shown in Fig. 5. The qualitative and quantitative agreement with the values obtained from the NMR experiments is within the 5% error. In all cases, the shape $D_{\mathrm{He}}(x_{\mathrm{He}})$ is correctly obtained in the molecular dynamics simulations, even for the subtle ^{3}He–^{4}He case. Although there is still significant noise in the computed diffusion coefficients, the substantial reduction due to the admixture of heavier and larger components is perfectly reproduced, hence supporting the experimental findings presented above.

Measured and simulated binary diffusion coefficient values can be compared with the classical theory for transport in dilute gases, the self diffusion and binary diffusion coefficients for gases of species 1 and 2, following the notation of ref. 7 is

$$D^0_{\mathrm{He,BG}} = \frac{3}{16} \frac{\sqrt{2\pi (k_{\mathrm{B}} T)^3 \left(\frac{1}{m_{\mathrm{He}}} + \frac{1}{m_{\mathrm{BG}}}\right)}}{P \pi \sigma^2_{\mathrm{He,BG}} \Omega^{(1,1)*}} \qquad (19)$$

where k_{B} is the Boltzmann constant, m_{He} and m_{BG} are the ^{3}He and BG atomic mass respectively, $\pi\sigma^2$ the collision cross section in a rigid-sphere model and $\Omega^{(1,1)*}$ a T-dependent factor depending on the actual interatomic potential.

The obtained values for the binary diffusion coefficient as well as the ^{3}He free diffusion coefficient obtained by NMR, by molecular dynamics simulations, and from eqn (19) are summarized in Table 1. Diffusion coefficient absolute values agree within 5%, which is within the individual error for each technique. In order to illustrate the decrease in He mobility caused by the buffer gases, the ratio of the free diffusion coefficient with each binary diffusion coefficient, R(BG) =

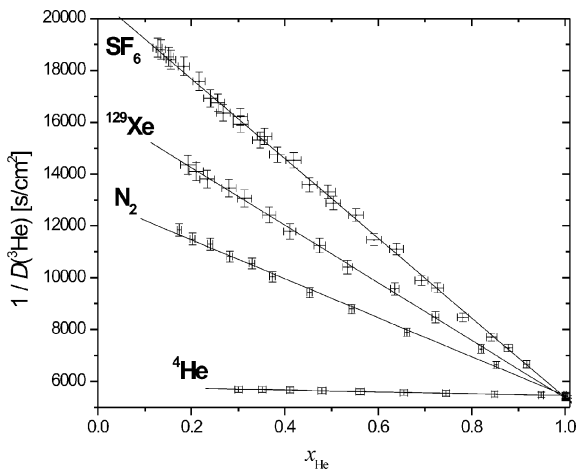

Fig. 4 ^{3}He diffusion coefficient obtained by NMR measurements as a function of the helium molar fraction, x_{He}, for binary mixtures corresponding to four different buffer gases (^{4}He, N_2, Xe and SF_6). The vertical error bars are the errors of the fitted diffusion coefficients, while the horizontal errors were estimated by eqn (14). The solid lines show the fits of eqn (18) to the data. The binary diffusion coefficients are found by extrapolating the fit to $x_{\mathrm{He}} = 0$. The obtained results are summarized in Table 1.

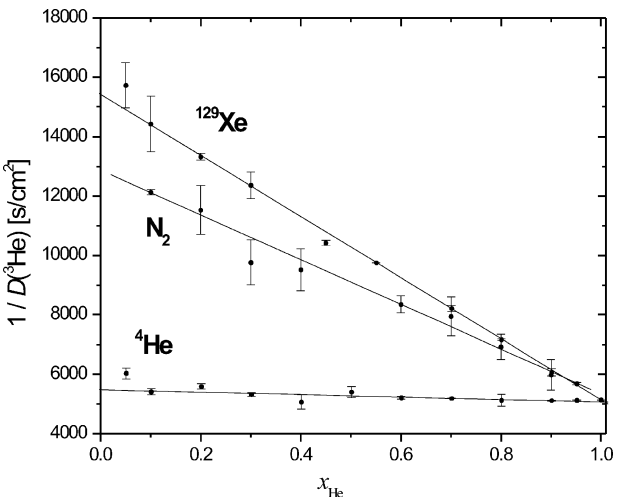

Fig. 5 ^{3}He diffusion coefficient obtained by simulations as a function of the helium molar fraction, x_{He}, for binary mixtures corresponding to three different buffer gases (^{4}He, N_2 and Xe). Error bars were estimated by comparing the diffusion coefficients obtained from the first and the second half of the simulation. The solid lines show the fits of eqn (18) to the data. The binary diffusion coefficients are found by extrapolating the fit to $x_{\mathrm{He}} = 0$. The obtained results are summarized in Table 1.

 This journal is © the Owner Societies 2006

Table 1 Diffusion coefficient of pure ^{3}He and binary diffusion coefficients ($D^0_{He/BG}$). Each column to the right of a buffer gas shows the ratio $R(BG) = D^0_{He/BG}/D_{He}$. Units are expressed in 10^{-4} m^2 s^{-1}

	^{3}He	^{4}He	$R(^4He)$	N_2	$R(N_2)$	Xe	R(Xe)	SF_6	$R(SF_6)$
NMR	1.85	1.72	0.94	0.77	0.42	0.61	0.34	0.48	0.26
Simulation	1.96	1.86	0.95	0.80	0.41	0.63	0.32	—	—
Eqn (19)	1.90	1.78	0.94	0.80	0.42	0.64	0.34	0.43	0.23

$D^0_{He/BG}/D_{He}$, is presented. The agreement between all three methods is very good.

Fig. 6 shows the inverse of the diffusion coefficient of ^{129}Xe upon a mixture with ^{3}He as well as the simulated data as a function of the ^{129}Xe molar fraction, x_{Xe}. Straight lines correspond to a linear fitting using the equation

$$\frac{1}{D_{Xe/He}(x_{Xe})} = \frac{x_{Xe}}{D_{Xe}} + \frac{1 - x_{Xe}}{D^0_{Xe/He}} \qquad (20)$$

where D_{Xe} is the self diffusion coefficient of ^{129}Xe and $D^0_{Xe/He}$ is the binary diffusion coefficient of the ^{129}Xe/^{3}He system. The obtained values together with the ratio $R'(He) = D^0_{Xe/He}/D_{Xe}$ and the theoretical values predicted by eqn (19) are listed in Table 2. A good agreement is obtained for the two experimental data sets with the theoretical prediction. There are some minor discrepancies where the simulated xenon diffusion coefficient at low Xe concentrations is slightly higher than the measured one.

One possible origin of these deviations around $x_{Xe} = 0.3$ are inhomogeneities of the Xe/He concentration within the sample volume. Local fluctuations or even gravity could cause a locally increased Xe concentration, whose Xe diffusion would be significantly reduced with respect to a perfectly homogeneous gas mixture with $x_{Xe} = 0.3$. This effect would correspond to an effective increase in the Xe mole fraction, hence bringing the experimental D_{Xe} closer to the simulated value. Additionally both experimental methods have increasing errors with decreasing numbers of observed particles, which might also add to this discrepancy. A further uncertainty is caused by the curvature of the inverse Xe diffusion coefficient

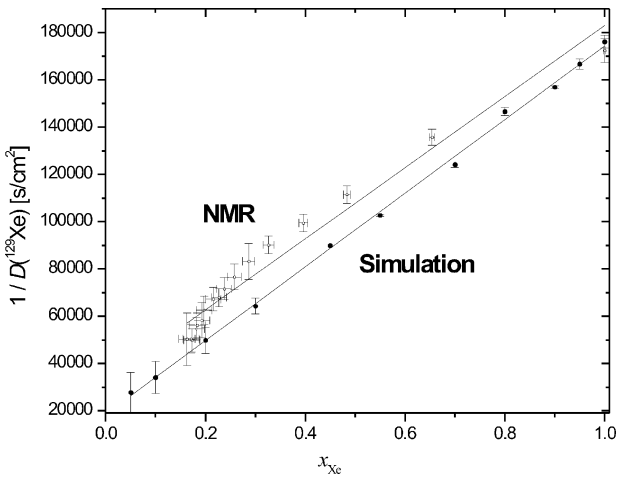

Fig. 6 ^{129}Xe diffusion coefficient obtained by NMR and simulations as a function of the xenon molar fraction, x_{He}, for the binary mixture ^{129}Xe–^{3}He. The solid lines show the fits of eqn (20) to the data. The obtained results are summarized in Table 2.

Table 2 Diffusion coefficient of pure ^{129}Xe, binary diffusion coefficient of the ^{129}Xe–^{3}He system, and the ratio $R'(He) = D^0_{Xe/He}/D_{Xe}$. Units are expressed in 10^{-4} m^2 s^{-1}

	^{129}Xe	^{3}He	R'(He)
NMR	0.058	0.307	5.29
Simulation	0.057	0.536	9.40
Eqn (19)	0.057	0.640	11.23
Eqn (21)	—	0.610	10.70

(see Fig. 6) at these lower concentrations, which complicates the extrapolation for $x_{Xe} \to 0$. Approximating the error due to this uncertainty gives a range for $1/D^0_{Xe/He}$ of 10^4 to 3×10^4 s cm^{-2}, resulting in a possible range for the binary diffusion coefficient of 3×10^{-5} to 10^{-4} m^2 s^{-1}.

The binary diffusion coefficient obtained by the simulation is about 16% lower than the theoretical value as computed from eqn (19). Higher approximations of the nth order to the diffusion coefficient take the form

$$\left[D^{(0)}_{1,2}\right]_k = D^0_{1,2} f^{(k)}_{1,2}. \qquad (21)$$

The function $f^{(2)}_{1,2}$ is a function of the molecular weights, the mole fractions, and the viscosities of the two gases, and also of the temperature. An explicit expression for this function which varies only slightly from unity can be found in Appendix A of ref. 7 and will not be reproduced here. Thus, the dependence of the binary diffusion coefficient on the composition of a mixture of gases is only slight. The second order corrected value is shown in Table 2, a reduction from $D^0_{Xe/He} = 6.4 \times 10^{-5}$ m^2 s^{-1} to $D^0_{Xe/He}(0) = 6.1 \times 10^{-5}$ m^2 s^{-1} is obtained, which is still higher from the simulated value by 12%.

Conclusions

In this paper an experimental setup and protocol for achieving a controlled binary gas mixture at ambient pressure is reported, in which one of the gas components is a noble LP gas. The gas mixing is controlled by pneumatic valves which are driven from the spectrometer, enabling a synchronized timing with the pulse sequences and complete automation of the experiment. The molar fraction determination is performed by direct inspection of the NMR signal assuming that the only source of loss of magnetization is produced by the RF excitation. This strategy turned out to be more accurate than other standard techniques for quantitative analysis of mixtures of gases with very different molar masses. This setup was then used for the measurement of the diffusion coefficient of ^{3}He as a function of its molar fraction in binary mixtures with four different inert buffer gases (^{4}He, N_2, Xe and SF_6) and for the measurement of ^{129}Xe diffusion coefficient as a function of its molecular fraction upon a mixture with ^{3}He.

The agreement between the experimentally measured diffusion coefficients with those obtained from molecular dynamics simulations and analytical expressions is very good, in particular for ^{3}He. The dependence of D(He/BG) on the molar concentration in mixtures with BG = N_2 and BG = Xe is neatly reproduced, illustrating the possibilities of fine-tuning diffusion properties of a gas by the admixture of another one of different molecular mass. In the case of the ^{129}Xe diffusion data, the agreement between experiment and simulation is somewhat less satisfactory. This might be due to the approximations in the Xe–Xe and Xe–He interaction potentials in the molecular dynamics simulations, but could also be explained by an imperfect experimental setup as discussed above. Presently, we are working on improving both aspects. Further studies may involve the possibility of running simulations in confined geometries, which would extend the applicability and increase the predictive power of the simulations, but also extension to mixtures of more than two components, for which the validity of a straightforward extension of eqn (20) is not trivial.

Acknowledgements

The authors want to thank Manfred Hehn and Hans-Peter Raich for their help in the design and construction of the gas handling system at the MPI-P, and Jörg Schmiedeskamp for assistance in hyperpolarizing ^{3}He. Furthermore, Stefan Appelt and Wolfgang Häsing (both Research Center Jülich, Germany) have to be acknowledged for designing and constructing the Xe-polarizer used for part of this work. Financial support by DFG (Forschergruppe ''Bildgestützte zeitliche und regionale Analyse der Ventilations—Perfusionsverhältnisse in der Lunge'', grant # FOR 474) and a special grant of the Max Planck society made this work possible.

References

1 B. M. Goodson, Nuclear Magnetic Resonance of Laser-Polarized Noble Gases in Molecules, Materials, and Organisms, *J. Magn. Reson.*, 2002, **155**, 157–216.
2 H. E. Möller, X. J. Chen, B. Saam, K. D. Hagspiel, G. A. Johnson, T. A. Altes, E. E. d. Lange and H.-U. Kauczor, MRI of the lungs using hyperpolarized noble gases, *Magn. Reson. Med.*, 2002, **47**, 1029–1051.
3 P. Callaghan and C. Eccles, Diffusion-limited resolution in nuclear magnetic resonance microscopy, *J. Magn. Reson.*, 1988, **78**, 1–8.
4 B. T. Saam, D. A. Yablonskiy, V. D. Kodibagkar, J. C. Leawoods, D. S. Gierada, J. D. Cooper, S. S. Lefrak and M. S. Conradi, MR Imaging of Diffusion of ^{3}He Gas in Healthy and Diseased Lungs, *Magn. Reson. Med.*, 2000, **44**, 174–179.
5 W. G. Schreiber, K. Markstaller, H.-U. Kauczor, B. Eberle, R. Surkau, G. Hanisch, A. Deninger, T. Grossmann, N. Weiler, E. Otten and M. Thelen, Ultrafast MR-Imaging of 3-Dimensional Distribution of Helium-3 Diffusion Coefficients in the Lung, in *International Society for Magnetic Resonance in Medicine, 7th Scientific Meeting*, Philadelphia, 1999, 2096.
6 X. J. Chen, H. E. Möller, M. S. Chawla, G. P. Cofer, B. Driehuys, L. W. Hedlund and G. A. Johnson, Spatially Resolved Measurements of Hyperpolarized Gas Properties in the Lung *In Vivo*. Part I: Diffusion Coefficient, *Magn. Reson. Med.*, 1999, **42**, 721–728.
7 J. Hirschfelder, C. Curtiss and R. Bird, *Molecular Theory of Gases and Liquids*, Wiley, New York, 1954.
8 C. P. Bidinosti, J. Choukeife, P.-J. Nacher and G. Tastevin, *In vivo* NMR of hyperpolarized ^{3}He in the human lung at very low magnetic fields, *J. Magn. Reson.*, 2003, **162**, 122–132.
9 G. Tastevin and P.-J. Nacher, NMR measurements of hyperpolarized ^{3}He gas diffusion in high porosity silica aerogels, *J. Chem. Phys.*, 2005, **123**, 064506.
10 R. W. Mair, D. Hoffmann, S. A. Sheth, G. P. Wong, J. P. Butler, S. Patz, G. P. Topulos and R. L. Walsworth, Reduced xenon diffusion for quantitative lung study–the role of SF_6, *NMR Biomed.*, 2000, **13**, 229–233.
11 J. C. Liner and S. Weissman, Determination of the Temperature Dependence of Gaseous Diffusion Coefficients Using Gas Chromatographic Apparatus, *J. Chem. Phys.*, 1972, **56**(5), 2288–2290.
12 P. S. Aurora and P. J. Dunlop, The pressure dependence of the binary diffusion coefficients of the systems He–Ar, He–N_2, He–O_2 and He–CO_2 at 300 and 323 K: Tests of Throne's equation, *J. Chem. Phys.*, 1979, **71**(6), 2430–2432.
13 R. H. Acosta, P. Blümler, S. Han, S. Appelt, F. W. Häsing, J. Schmiedeskamp, W. Heil and H. W. Spiess, Imaging of a mixture of hyperpolarized ^{3}He and ^{129}Xe, *Magn. Reson. Imaging*, 2004, **22**, 1077–1083.
14 R. H. Acosta, P. Blümler, L. Agulles-Pedrós, A. E. Morbach, J. Schmiedeskamp, A. Herweling, U. Wolf, A. Scholz, W. G. Schreiber, W. Heil, M. Thelen and H. W. Spiess, Controlling the Diffusion of ^{3}He by Buffer Gases as a Structural Contrast Agent in Lung MRI, *J. Magn. Reson. Imaging*, 2006, in press.
15 E. J. R. van Beek, J. Schmiedeskamp, J. M. Wild, M. N. J. Paley, F. Filbir, S. Fichele, F. Knitz, G. H. Mills, N. Woodhouse, A. Swift, W. Heil, M. Wolf and E. W. Otten, Hyperpolarized3-helium MR imaging of the lungs: testing the concept of a central production facility, *Eur. Radiol.*, 2003, **13**, 2583–2586.
16 J. Becker, W. Heil, B. Krug, M. Leduc, M. Meyerhoff, P. J. Nacher, E. W. Otten, T. Prokscha, L. D. Schearer and R. Surkau, Study of mechanical compression of spin-polarized 3He gas, *Nucl. Instrum. Methods Phys. Res., Sect. A*, 1994, **346**, 45–51.
17 N. J. Shah, T. Ünlü, H. P. Wegner, H. Halling, K. Zilles and S. Appelt, Measurement of rubidium and xenon absolute polarization at high temperatures as a means of improved production of hyperpolarized ^{129}Xe, *NMR Biomed.*, 2000, **13**, 214–219.
18 H. Raich and P. Blümler, Design and construction of a dipolar Halbach array with a homogeneous field from identical bar magnets: NMR Mandhalas, *Concepts Magn. Reson., Part B*, 2004, **23B**, 16–25.
19 P. T. Callaghan, *Principles of Nuclear Magnetic Resonance Microscopy*, Clarendon Press, Oxford, 1991.
20 E. O. Stejskal and J. E. Tanner, Spin Diffusion Measurements: Spin Echoes in the Presence of a Time-Dependent Field Gradient, *J. Chem. Phys.*, 1965, **42**, 288.
21 H. E. Möller, X. J. Chen, M. S. Chawla, B. Driehuys, L. W. Hedlund and G. A. Johnson, Signal Dynamics in Magnetic Resonance Imaging of the Lung with Hyperpolarized Noble Gases, *J. Magn. Reson.*, 1998, **135**, 133–143.
22 J.-H. Gao, L. Lemen, J. Xiong, B. Paytal and P. T. Fox, Magnetization and diffusion effects in NMR imaging of hyperpolarized substances, *Magn. Reson. Med.*, 1997, **37**, 153–158.
23 G. A. Johnson, G. Cates, X. J. Chen, G. P. Cofer, B. Driehuys, W. Happer, L. W. Hedlund, B. Saam, M. D. Shattuck and J. Swartz, Dynamics of magnetization in hyperpolarized gas MRI of the lung, *Magn. Reson. Med.*, 1997, **38**, 66–71.
24 E. Lindahl, B. Hess and D. v. d. Spoel, GROMACS 3.0: A package for molecular simulation and trajectory analysis, *J. Mol. Model.*, 2001, **7**, 306–317.
25 R. C. Reid, J. M. Prausnitz and B. E. Poling, *The Properties of Gases and Liquids*, McGraw-Hill Book Company, New York, 4th edn, 1987.

 This journal is © the Owner Societies 2006